



1           **Development of high spatial resolution annual**  
2           **emission inventory of greenhouse gases from open**  
3           **straw burning in Northeast China from 2001 to 2020**

4           Zihan Song<sup>a,b</sup>, Leiming Zhang<sup>c</sup>, Chongguo Tian<sup>d</sup>, Qiang Fu<sup>a,b</sup>, Zhenxing Shen<sup>e</sup>,  
5                                   Renjian Zhang<sup>f</sup>, Dong Liu<sup>a,b</sup>, Song Cui<sup>a,b\*</sup>

6           <sup>a</sup> *International Joint Research Center for Persistent Toxic Substances (IJRC-PTS), School of*  
7           *Water Conservancy and Civil Engineering, Northeast Agricultural University, Harbin,*  
8           *Heilongjiang 150030, China*

9           <sup>b</sup> *Research Center for Eco-Environment Protection of Songhua River Basin, Northeast*  
10           *Agricultural University, Harbin, Heilongjiang 150030, China*

11           <sup>c</sup> *Air Quality Research Division, Science and Technology Branch, Environment and Climate*  
12           *Change Canada, Toronto, Ontario M3H 5T4 Canada*

13           <sup>d</sup> *CAS Key Laboratory of Coastal Environmental Processes and Ecological Remediation,*  
14           *Yantai Institute of Coastal Zone Research, Chinese Academy of Sciences, Shandong Key*  
15           *Laboratory of Coastal Environmental Processes, YICCAS, Yantai 264003, China*

16           <sup>e</sup> *Department of Environmental Sciences and Engineering, Xi'an Jiaotong University, Xi'an,*  
17           *710049, China*

18           <sup>f</sup> *Institute of Atmospheric Physics, Chinese Academy of Sciences, Beijing 100029, China*

19           \*Corresponding author: Dr. Song Cui           Email: cuisong-bq@neau.edu.cn (S. Cui)

20

21

22

23           **WORD COUNT: 4800**

24           **6 FIGURES**

25           **1 TABLE**



## 26 **Abstract**

27 Open straw burning has been widely recognized as a significant source of greenhouse  
28 gases (GHGs), posing critical risks to atmospheric integrity and potentially  
29 exacerbating global warming. In this study, we proposed a novel method that integrates  
30 crop cycle information into extraction and classification of fire spots from open straw  
31 burning in Northeast China from 2001 to 2020. By synergizing the extracted fire spots  
32 with the modified Fire Radiative Power (FRP) algorithm, we developed high spatial  
33 resolution emission inventories of GHGs, including carbon dioxide (CO<sub>2</sub>), methane  
34 (CH<sub>4</sub>), and nitrous oxide (N<sub>2</sub>O). Results showed that the northern Sanjiang Plain,  
35 eastern Songnen Plain, and eastern Liao River Plain were areas with high intensity of  
36 open straw burning. The number of fire spots was elevated during 2013-2017,  
37 accounting for 58.0% of the total fire spots observed during 2001-2020. The prevalent  
38 season for open straw burning shifted from autumn (pre-2016) to spring (post-2016),  
39 accompanied by a more dispersed pattern in burning dates. The two-decade cumulative  
40 emissions of CO<sub>2</sub>, CH<sub>4</sub>, and N<sub>2</sub>O were quantified at 202 Tg, 568 Gg, and 16.0 Gg,  
41 respectively, amounting to 221 Tg of CO<sub>2</sub>-eq. Significant correlations were identified  
42 between GHGs emissions and both straw yields and straw utilization ( $p < 0.01$ ). The  
43 enforcement of straw burning bans since 2018 has played a pivotal role in curbing open  
44 straw burning, and reduced fire spots by 50.7% on annual basis compared to 2013-2017.  
45 The novel method proposed in this study considerably enhanced the accuracy in  
46 characterizing spatiotemporal distributions of fire spots from open straw burning and



47 quantifying associated pollutants emissions.

48 **Keywords:** Open straw burning; Fire spot; Crop cycle; Greenhouse gas; Emission

49 inventory

50 **Keywords Plus:** Open straw burning; MODIS; Fire spot; Accurate extraction; Crop

51 cycle; Crop type; Phenology; Greenhouse gas; Emission inventory; Driving factor;

52 Policy

53



54 **1 Introduction**

55 Open straw burning, a customary practice in agricultural areas, serves multiple purposes,  
56 including rapid straw disposal, weed control, nutrient release, and pest management  
57 (Korontzi et al., 2006; Wen et al., 2020). This practice results in short-term yet intense  
58 emissions of greenhouse gases (GHGs), such as carbon dioxide (CO<sub>2</sub>), methane (CH<sub>4</sub>),  
59 and nitrous oxide (N<sub>2</sub>O). The accumulation of these gases in the atmosphere adversely  
60 impacts climate and atmospheric chemistry (Weldemichael and Assefa, 2016; Tang et  
61 al., 2020; Hong et al., 2023). To date, open straw burning remains to be prevalent in  
62 grain-producing areas globally, despite the many drawbacks of such a practice (Gadde  
63 et al., 2009; Huang et al., 2013; Zhu et al., 2015; Ahmed et al., 2019; Mehmood et al.,  
64 2020; Fu et al., 2022; Xu et al., 2023a). Thus, accurate and high spatial resolution  
65 emission inventories for GHGs from this source sector are needed from regional to  
66 global scales to assess potential climate and air quality impacts and formulate carbon  
67 mitigation policies.

68

69 The “bottom-up” approach, which is based on the amount of straw burned and  
70 corresponding emission factors, has been widely employed to establish emission  
71 inventories for various pollutants emitted from open straw burning (van der Werf et al.,  
72 2017; Wang et al., 2018; Liu et al., 2021; Zheng et al., 2023). Emission factors for  
73 diverse pollutants released from different types of straw burning have been extensively  
74 investigated in laboratory studies (Li et al., 2007; Liu et al., 2011; Stockwell et al., 2014;



75 Pan et al., 2017; Peng et al., 2016; Sun et al., 2016). However, estimation of the amount  
76 of straw burned is subject to large uncertainties since it involves many parameters, such  
77 as grain yield, ratio of straw and grain, open burning proportion, burning efficiency,  
78 and dry matter fraction (Guan et al., 2017; Zhou et al., 2017). Consequently, existing  
79 regional-scale emission inventories based on the “bottom-up” approach generally have  
80 large uncertainties and low spatiotemporal resolutions (Tian et al., 2011; Jin et al., 2017).

81

82 The advent of satellite technologies, such as Moderate Resolution Imaging  
83 Spectroradiometer (MODIS, remote sensing instrument), Visible Infrared Imaging  
84 Radiometer Suite (VIIRS, remote sensing instrument), and Himawari-8 (geostationary  
85 satellite), has markedly revolutionized the monitoring of open straw burning, enabling  
86 real-time and high spatiotemporal resolution fire spot products to be accessible to the  
87 general public (Schroeder et al., 2014; Giglio et al., 2016; Xu et al., 2017; Wu et al.,  
88 2018; Zhuang et al., 2018; Lv et al., 2024). Many studies have effectively utilized the  
89 satellite fire spot products for constructing emission inventories, based on either the  
90 burned area or fire spot counts (FC) (Jin et al., 2018; Ke et al., 2019; Li et al., 2019;  
91 Zhang et al., 2019; Cui et al., 2021), and have improved the spatiotemporal resolutions  
92 of the emission inventories (Wu et al., 2023). With continuous enrichment of satellite  
93 data, a strong relationship was observed between fire radiative power (FRP) and  
94 emission amounts from open straw burning (Wu et al., 2023). Consequently, the FRP  
95 algorithm has been widely accepted for estimating emissions (Wooster et al., 2005;



96 Freeborn et al., 2008; Vermote et al., 2009; Yang et al., 2019). More recently, Yang et  
97 al. (2020) improved the FRP algorithm by calibrating the contributions of open straw  
98 burning to ground observation data based on model simulation results using the coupled  
99 Weather Research and Forecasting model and Community Multiscale Air Quality  
100 (WRF-CMAQ) model.

101

102 At present, the identification of straw types in open straw burning typically relies on  
103 crop data, such as the International Geosphere-Biosphere Programme (IGBP)-Modified  
104 MODIS Land Use and MapSPAM datasets (Ke et al. 2019; Yang et al. 2020). These  
105 low spatiotemporal resolution crop data contribute to errors in both the extraction of  
106 fire spots and the identification of straw types (Ke et al., 2019; Liu et al., 2022).  
107 Additional errors come from planting structure adjustment and frequent variations in  
108 crop phenology. For instance, fire spots occurred during crop growth might be  
109 incorrectly classified as open straw burning, while those occurred prior to crop growth  
110 could be inaccurately attributed to burning of straws from subsequent harvests (Zhou  
111 et al., 2022). Therefore, high spatiotemporal resolution data on crop types and  
112 phenology are critical, and such data should be integrated into the extraction and  
113 classification of fire spots from open straw burning to accurately estimate emissions of  
114 various pollutants from this source sector.

115

116 To control emissions from open straw burning, the “Air Pollution Prevention and



117 Control Action Plan” (APPCAP) took into effect in 2013 in China (Huang et al., 2021).  
118 In addition, China committed to achieve carbon peak by 2030 and carbon neutrality by  
119 2060, which draws unprecedented challenges in reducing carbon emissions from open  
120 straw burning (Wu et al., 2023). As a significant grain-producing region in China,  
121 Northeast China produced 135 million tons of major grains (corn, rice, beans, and wheat)  
122 in 2020, accounting for 21.4% of total production in China (National Bureau of  
123 Statistics of China, 2021). During 2013-2018, open straw burning in Northeast China  
124 exhibited an increasing trend, while decreasing in all other regions of China (Huang et  
125 al., 2021). The constant increase reflects the expansion of the agricultural sector and  
126 economic development in Northeast China yet relatively unconstrained open burning  
127 activities (Huang et al., 2021). Liu et al. (2022) estimated CO<sub>2</sub> emissions from open  
128 straw burning in Northeast China as high as 344 Tg from 2012 to 2020.

129

130 In this study, high spatial resolution fire spot products were used to develop annual  
131 emission inventories of GHGs, including CO<sub>2</sub>, CH<sub>4</sub>, and N<sub>2</sub>O, from open straw burning  
132 in Northeast Chian for the period of 2001-2020. To improve the accuracy of the  
133 developed emission inventory, a novel concept that integrates the crop cycle  
134 information into fire spot extraction and classification was adopted. Furthermore, this  
135 study conducted a thorough analysis to assess the driving factors influencing GHGs  
136 emissions during the two decades. This study comprehensively examined GHGs  
137 emissions from open straw burning in Northeast China and offered valuable insights to



138 policy makers for mitigating carbon emissions and air pollution in agricultural areas.

## 139 **2 Methodology**

### 140 **2.1 Extraction and classification of fire spots**

141 The MODIS fire product (MCD14ML, Collection 6.0 Process Version 3) was selected  
142 from 1 January 2001 to 31 December 2020 for the whole region of Northeast China.  
143 MCD14ML shows active fire detections and thermal anomalies, including forest fires,  
144 grass fires, and open straw burning. The spatial resolution of the dataset is about 1 km<sup>2</sup>,  
145 and essential variables, such as latitude, longitude, acquisition date and time (in UTC),  
146 and FRP, among others, were available (Giglio et al., 2016,  
147 <https://firms.modaps.eosdis.nasa.gov/>).

148

149 This study selected ChinaCropArea1 km and ChinaCropPhen1 km datasets to extract  
150 and classify fire spots from open straw burning (Luo et al., 2020a; Luo et al., 2020b).  
151 These datasets present annual data on the type and phenology (Day of Year (Doy) of  
152 emergence and maturity) of grain crops (corn, rice, and wheat), respectively.  
153 Considering that Northeast China is a major bean-producing area, we also compiled  
154 bean distribution datasets (Li et al., 2021; Xuan et al., 2023). There are some gaps in  
155 these datasets compared to the comprehensive information required for this study, as  
156 detailed in **Table S1**.

157



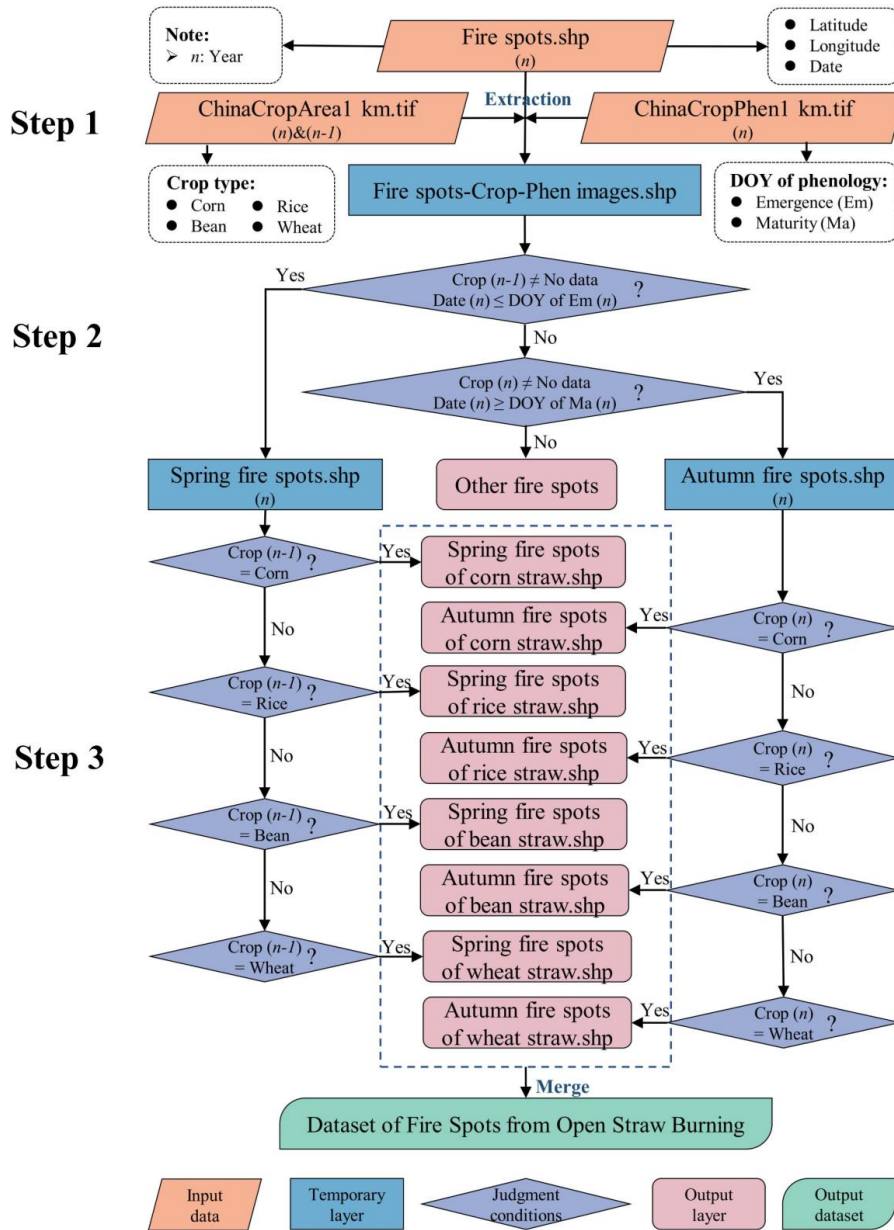


158 **Fig. 1** describes the meticulous process to accurately extract and classify fire spots from  
159 open straw burning in areas experiencing one-harvest season every year. The process  
160 involves several key steps:

161 **Step 1)** The current year's ChinaCropPhen1 km and ChinaCropArea1 km, along with  
162 the previous year's ChinaCropArea1 km data, were extracted to Fire spots (MCD14ML)  
163 by ArcGIS 10.2 software, to obtain the Fire spots-Crop-Phen dataset.

164 **Step 2)** Considering the crop cycle, the extraction of fire spots was divided into two  
165 stages. The first stage is before crop growth (spring) and requires the fire spot to satisfy  
166 two conditions: a) there was a crop planted in the previous year, and b) the burning date  
167 is before emergence. The second stage is after crop growth (autumn) and also involves  
168 two conditions: a) there was a crop planted in the current year, and b) the burning date  
169 is after maturity.

170 **Step 3)** For fire spots in spring, the type of straw burned is identified based on the  
171 previous year's crop type. For autumn fire spots, the straw type is determined according  
172 to the crop type of the current year.



173

174 **Fig. 1** Extraction and classification method for fire spots from open straw burning



175 **2.2 Development of high spatial resolution emission inventories for GHGs and**  
176 **exploration of driving factors**

177 Annual emission inventories for GHGs were developed for the region of Northeast  
178 China at a grid resolution of 5 km × 5 km for the years 2001 to 2020. The domain grids  
179 were created using Fishnet of ArcGIS 10.2 software.

180

181 The modified FRP algorithm (Yang et al., 2020) is used to estimate the emissions of  
182 GHGs from open straw burning in this study:

183 
$$E = \alpha \times \int_{t_1}^{t_2} FRP^* dt \times \beta \times F = \alpha \times FRP \times f_{FRP} \times (t_2 - t_1) \times \beta \times F \quad (1)$$

184 where  $E$  (in g) is the emissions of GHGs;  $\alpha$  is a correction factor to adjust for satellite  
185 data errors and a value of 2.5 is used here (Vadrevu and Lasko, 2018);  $t_1$  and  $t_2$  are the  
186 beginning and ending time of fire spots, respectively, and the average burning time (3  
187 hours) of a fire spot in Northeast China was obtained by delivering questionnaires to  
188 local farmers (Yang et al., 2020);  $FRP^*$  (in MW) is adjusted satellite detected  $FRP$ ;  $FRP$   
189 (in MW) is the instantaneous  $FRP$  observed by satellite;  $f_{FRP}$  is a correction factor that  
190 is used for adjusting the underestimated emissions by fire spots and an optimal value  
191 of 5 was obtained for  $f_{FRP}$  by Yang et al. (2020);  $\beta$  (in kg·MJ<sup>-1</sup>) is biomass combustion  
192 rate and the average value of 0.411 kg·MJ<sup>-1</sup> from previous studies is used here (Wooster  
193 et al., 2005; Freeborn et al., 2008); and  $F$  (in g·kg<sup>-1</sup>) is the emission factor for individual  
194 straw type (**Table 1**) (Li et al., 2007; Liu et al., 2011; Peng et al., 2016).

195



196 **Table 1.** Emission factors of open straw burning for different crop types

Crop	Emission factors ( $\text{g}\cdot\text{kg}^{-1}$ )		
	CO <sub>2</sub>	CH <sub>4</sub>	N <sub>2</sub> O
Corn	1350	4.4	0.12
Rice	1460	3.2	0.11
Bean	1445	3.9	0.09
Wheat	1460	3.4	0.05

197

198 Driving factors such as the output of major grains and rural residential coal  
199 consumption for temporal variations of annual GHGs emissions were explored through  
200 Pearson correlation analysis using SPSS 20.0. Information on the above data is also  
201 detailed in **Table S1**.

### 202 **3 Results and discussion**

#### 203 **3.1 Spatial and temporal distributions of fire spots**

204 Cultivated lands in Northeast China primarily distribute in Sanjiang Plain (Northeast  
205 Heilongjiang Province), Songnen Plain (West Heilongjiang Province and Midwest Jilin  
206 Province), and Liao River Plain (Central Liaoning Province) (**Fig. 2(a)**). Fire spots were  
207 widely spread, covering most cultivated lands, including both dry and paddy fields  
208 across Northeast China (**Fig. 2(a)** and **2(b)**). A total of 160,583 fire spots from open  
209 straw burning were recorded during 2001-2020. Note that traditional methods that do  
210 not consider crop cycle overestimated the total number of fire sports by 8686 over the  
211 20-year period, with the largest error in 2017 (an overestimation of 4300) (**Fig. 2(c)**).  
212 This highlights the importance of integrating crop cycle information into fire spot



213 extraction for open straw burning to enhance data accuracy and reliability. Considering  
214 the 20-year together (2001-2020), high occurrence frequencies of open straw burning  
215 (also referred to as intensity of fire spots below) appeared in the northern Sanjiang Plain,  
216 eastern Songnen Plain, and eastern Liao River Plain, as well as scattered areas close to  
217 Inner Mongolia (**Fig. 2(a)** and **2(b)**).

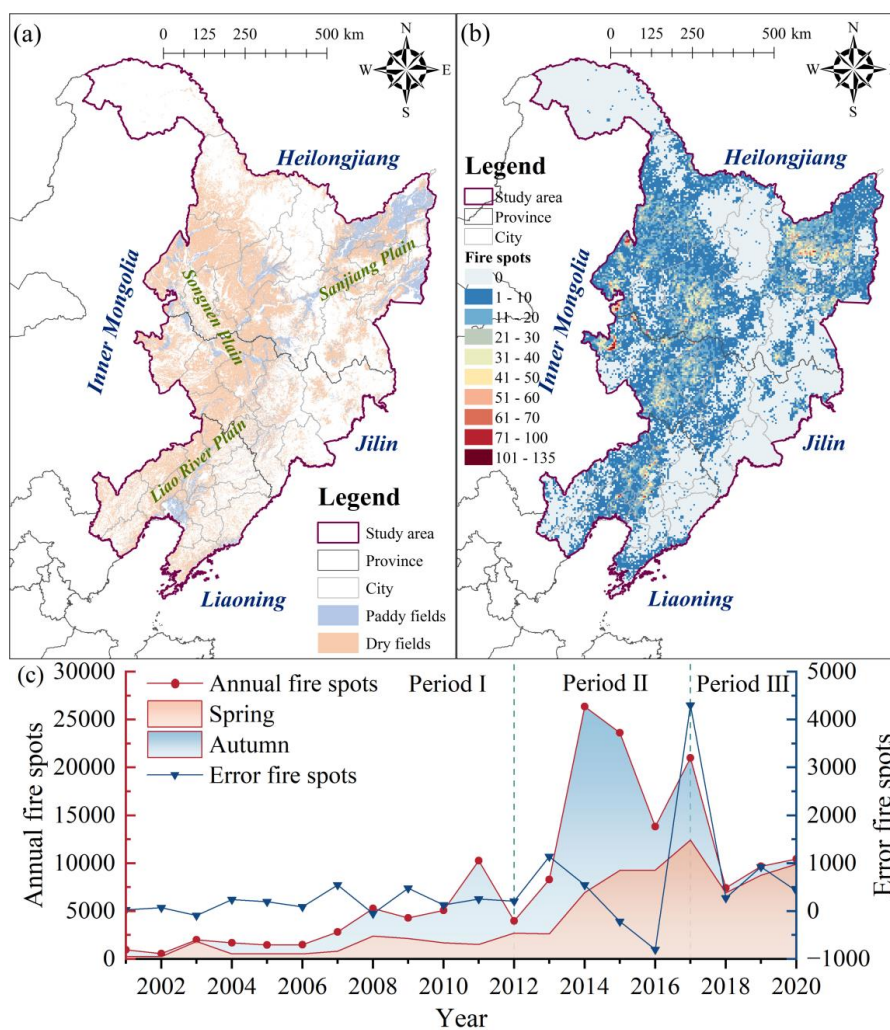
218

219 Interannual variations of fire spots distributions are shown in **Fig. S1**. In the Sanjiang  
220 Plain, low occurrence frequencies of fire spots were observed in a few cultivated lands  
221 during 2001-2006 (**Fig. S1(a)** to **Fig. S1(f)**) and in most cultivated lands in the northern  
222 part of the Plain during 2007-2013 (**Fig. S1(g)** to **Fig. S1(m)**). Note that in 2014 and  
223 later years, fire spots were extended to the entire Sanjiang Plain, and the northern part  
224 of the Plain became an area with high intensity of fire spots (**Fig. S1(n)** to **Fig. S1(q)**),  
225 although a few cultivated lands in this Plain recorded low intensity of fire spots after  
226 2018 (**Fig. S1(r)** to **Fig. S1(t)**). In the Songnen Plain, most cultivated lands recorded  
227 fire spots during 2014 to 2017, with highest intensity in the northern and eastern parts  
228 of the Plain (**Fig. S1(n)** to **Fig. S1(q)**). The occurrence frequencies of fire spots  
229 decreased across the plain since 2018, particularly in the northern part of the Plain (**Fig.**  
230 **S1(r)** to **Fig. S1(t)**). In the Liao River Plain, although fire spots were observed in most  
231 cultivated lands in the eastern part of the Plain during 2014-2017, high occurrence  
232 frequency was only recorded in 2014 (**Fig. S1(n)** to **Fig. S1(q)**).

233



234 Apparently, open straw burning events decreased in all of the three Plains since 2018  
 235 (Fig. S1(r) to Fig. S1(t)), which was likely due to the intensified effort from the Chinese  
 236 government banning open straw burning (Hong et al., 2023). Furthermore, the  
 237 reduction in the number of fire spots was more significant in the Sanjiang Plain and  
 238 northern Songnen Plain than Liao River Plain (Fig. S1), indicating more compliance  
 239 with straw burning bans from State Farms in the former two regions.



240



241 **Fig. 2** (a) Spatial distributions of cultivated land in 2020 in Northeast China  
242 (<https://www.resdc.cn>), (b) spatial distributions of the total number of fire spots during 2001-  
243 2020 in Northeast China, and (c) seasonal distributions and errors (error = misclassification -  
244 corrected classification) of the annual fire spots from 2001 to 2020.

245

246 Fire spots from open straw burning concentrated in spring and autumn, with few  
247 burning events in the other two seasons in Northeast China. Open straw burning events  
248 in this region during 2001-2020 can be roughly divided into three distinctive periods  
249 (**Fig. 2(c)**). During **Period I** (2001-2012), the annual average number of fire spots in  
250 this region was 3,328. There were more fire spots in autumn than spring in most of  
251 these years. During **Period II** (2013-2017), there was a substantial surge in fire spots,  
252 with an annual average of 18,622 spots, accounting for 58.0% of the 20-year total.  
253 Notably, the number of fire spots peaked at 26,359 in 2014. Spring fire spots  
254 consistently increased annually, reaching the highest in 2017 at 12,419 spots. The  
255 variations for autumn fire spots were fluctuating, with a peak of 19,408 spots in 2014.  
256 During 2013-2015, autumn fire spots were higher than spring; however, this trend  
257 reversed in 2016 and 2017, with spring fire spots becoming more dominant. During  
258 **Period III** (2018-2020), the number of fire spots experienced a significant decrease,  
259 averaging 9,178 spots annually, which was a 50.7% decrease from **Period II**. Spring  
260 emerged as the primary season of fire spots, accounting for approximately 92.8% of the  
261 annual total. Zhao et al. (2021) have reported a similar phenomenon, in which the

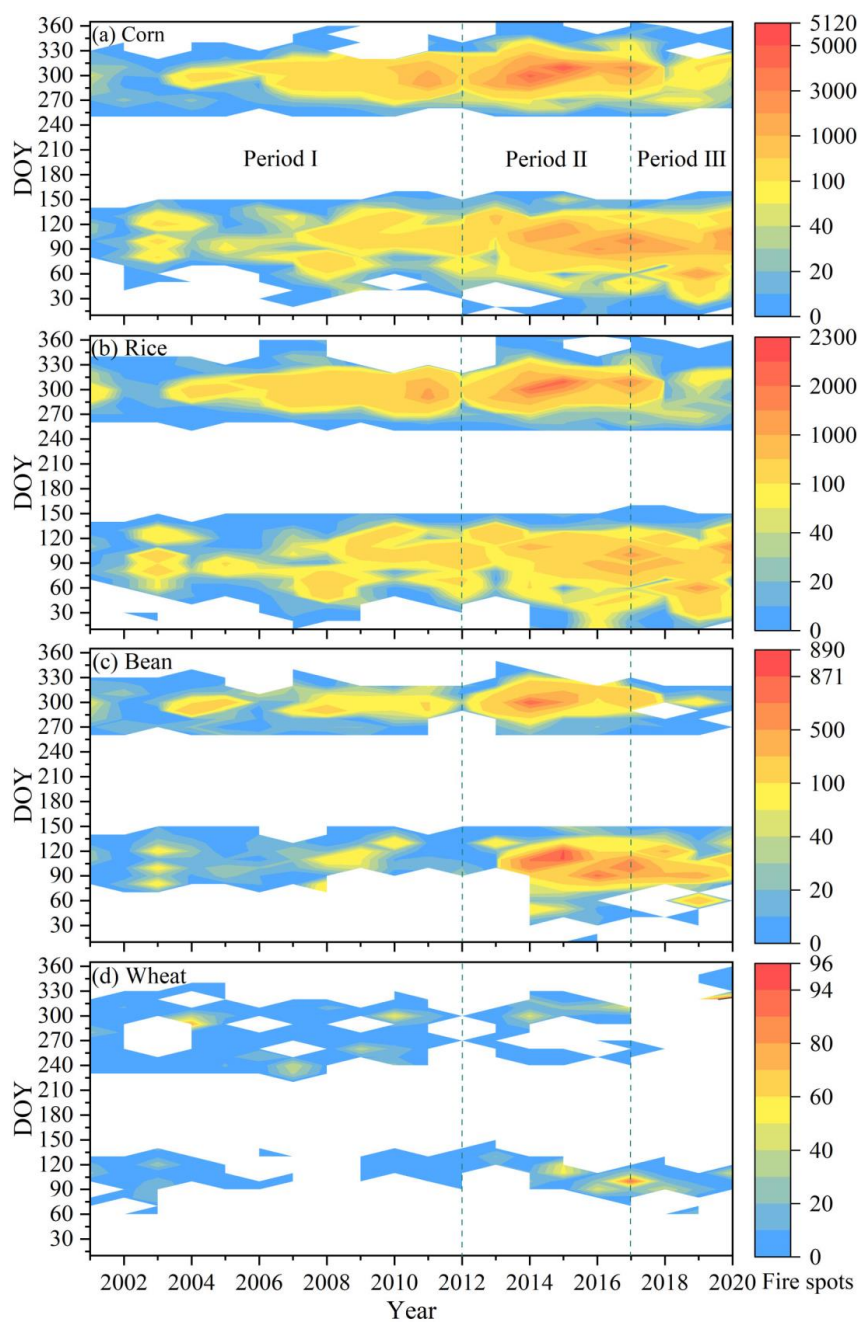


262 primary season of open straw burning in Northeast China gradually shifts to spring  
263 (April to June). The apparent seasonal variations of open straw burning primarily stems  
264 from strict government bans imposed after the autumn harvest (Yang et al., 2020). In  
265 addition, farmers' increasing awareness regarding how open straw burning contributes  
266 to the thawing of spring soil may also be a factor (Saxton et al., 1993; Song et al., 2023).  
267  
268 The burning dates of straw in Northeast China also changed during the three periods,  
269 besides varying with crop type. During **Period I** (2001-2012), the autumn burning dates  
270 of corn, rice, and bean straw were concentrated from late September to mid-November  
271 (DOY range of 270 to 320) (**Fig. 3(a)** to **Fig. 3(c)**). Spring burning dates of corn and  
272 rice straw were concentrated between mid-March and mid-May (DOY range of 80 to  
273 140) in 2001, while dispersed to late February to mid-May (DOY range of 60 to 140)  
274 in 2012 (**Fig. 3(a)** and **Fig. 3(b)**). However, no significant dispersal trend was found for  
275 spring burning dates of bean straw (**Fig. 3(c)**). During **Period II** (2013-2017), the  
276 dispersion of spring burning dates for corn, rice, and bean straws became more  
277 pronounced, extending from early February to mid-May (DOY range 40 to 140) (**Fig.**  
278 **3(a)** to **Fig. 3(c)**). During **Period III** (2018-2020), the dispersion of spring burning dates  
279 for corn, rice, and bean straws persisted (**Fig. 3(a)** to **Fig. 3(c)**). Unlike other crops, the  
280 burning dates for wheat straw did not conform to the aforementioned pattern of  
281 variation, likely due to a limited number of fire spots (**Fig. 3(d)**). The changing  
282 dispersion of burning dates for each crop type indicates shifts in agricultural practices





283 that may be influenced by regional straw burning ban policies, environmental  
284 conditions, and farming practices (Yang et al., 2020).



285



286 **Fig. 3** The frequency distribution of burning dates of various straws: (a), (b), (c), and (d)  
287 represent corn, rice, bean, and wheat straw, respectively.

### 288 **3.2 High spatial resolution annual emission inventory of GHGs**

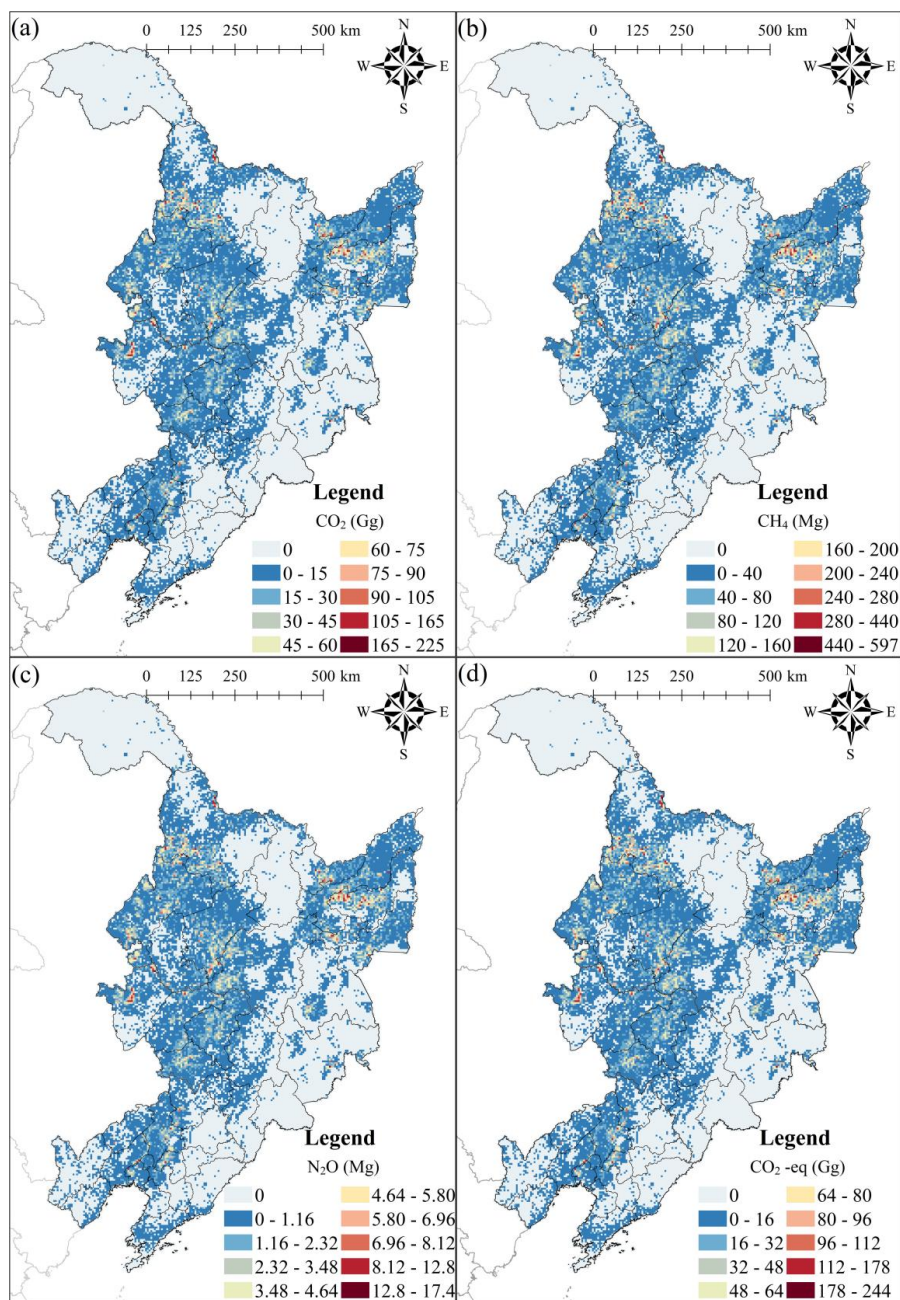
289 The cumulative emissions of CO<sub>2</sub>, CH<sub>4</sub>, and N<sub>2</sub>O from open straw burning in Northeast  
290 China from 2001 to 2020 amounted to 202 Tg, 568 Gg, and 16.0 Gg, respectively (or  
291 221 Tg CO<sub>2</sub>-eq in total). The spatial distributions of GHGs emissions correspond well  
292 with those of fire spots, particularly in high emission areas (**Fig. 2** and **Fig. 4**). However,  
293 the amounts of GHGs emissions in the northern Songnen Plain unexpectedly exceeded  
294 those in the eastern Songnen Plain and eastern Liao River Plain, suggesting that even  
295 low intensity fire spots can generate considerable emissions of GHGs due to higher  
296 FRP detected via remote sensing. Therefore, the FRP algorithm proves more effective  
297 than burned areas-based algorithms in identifying emission intensity resulted from open  
298 straw burning while reducing the uncertainty associated with high spatiotemporal  
299 resolution emission inventory (Wu et al., 2023).

300

301 The annual emissions of CO<sub>2</sub>, CH<sub>4</sub>, N<sub>2</sub>O, and CO<sub>2</sub>-eq from 2001 to 2020 are presented  
302 in **Figs. S2, S3, S4, and S5**, respectively. The spatiotemporal patterns of GHGs  
303 emissions correspond well to the observed trends in fire spots during **Period I** (2001-  
304 2012). However, during **Period II** (2013-2017) and **Period III** (2018-2020), the  
305 emissions of GHGs in the eastern Songnen Plain and eastern Liao River Plain did not  
306 exhibit a proportional increase with the rise in fire spots. This discrepancy can be



307 attributed to the dispersed burning dates among individual farmers in these regions,  
308 resulting in high intensity fire spots with relatively low emissions. In contrast, several  
309 State Farms located in the northern Sanjiang Plain and northern Songnen Plain  
310 demonstrated a higher level of synchronization in open straw burning activities,  
311 resulting in parallel trends between fire spots and emissions (Cui et al., 2021).



312

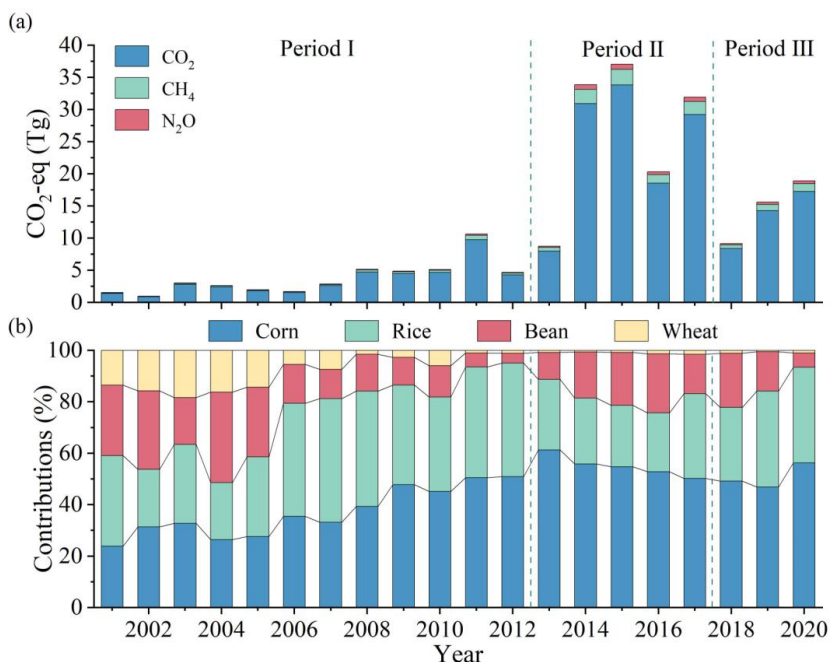
313 **Fig. 4** The cumulative GHGs emissions from open straw burning in Northeast China from 2001

314 to 2020: (a)-(d) for CO<sub>2</sub>, CH<sub>4</sub>, N<sub>2</sub>O, and CO<sub>2</sub>-eq emissions, respectively.

315



316 During **Period I** (2001 - 2012), average annual CO<sub>2</sub>-eq emission was at 3.75 Tg, and  
317 the cumulative CO<sub>2</sub>-eq emission amounted to 45.1 Tg. During **Period II** (2013 - 2017),  
318 average annual CO<sub>2</sub>-eq emission increased substantially to 26.4 Tg, and the cumulative  
319 emission during this period amounted to 132 Tg, which accounted for 59.8% of the total  
320 emissions over the two decades. During **Period III** (2018 - 2020), average annual CO<sub>2</sub>-  
321 eq emissions decreased significantly to 14.6 Tg, and the cumulative emission during  
322 this period amounted to 43.7 Tg (**Fig. 5(a)**). The trend of CO<sub>2</sub>-eq emission from 2001  
323 to 2020 generally corresponds with the occurrence of fire spots, except for 2015 when  
324 higher emissions were obtained despite having fewer fire spots than the case in 2014  
325 (**Fig. 5(a)**). Such a trend is consistent with those of carbonaceous gases and aerosols  
326 (CGA) emissions estimated by Liu et al., (2022). This discrepancy between fire spots  
327 and pollutant emissions in 2015 highlights the limitations of estimating pollutant  
328 emissions based solely on burned areas (Ke et al., 2019; Wu et al. 2023). The  
329 combustion of corn and rice straw was identified as the primary contributors to CO<sub>2</sub>-eq  
330 emissions, accounting for 51.0% and 30.9% of the total emissions, respectively (**Fig.**  
331 **5(b)**). Specifically, corn straw burning released 101.6, 8.28, and 2.69 Tg, while rice  
332 straw burning released 126.8, 6.95, and 2.85 Tg of CO<sub>2</sub>, CO<sub>2</sub>-eq for CH<sub>4</sub>, and CO<sub>2</sub>-eq  
333 for N<sub>2</sub>O, respectively.  
334



335

336 **Fig. 5** (a) Reginal total annual CO<sub>2</sub>-eq emissions and (b) percentage contributions from open

337 burning of individual crop straw type.

338

339 Our estimated CO<sub>2</sub> emission for 2013 in Northeast China (7989.3 Gg) was slightly

340 higher than that estimated from the Fire Inventory from NCAR version 1.5 (FINNv1.5)

341 (5936.6 Gg) by Mehmood et al. (2018), which was likely because FINNv1.5

342 underestimated the open biomass burning in China (Stavrou et al., 2016; Yang et al.,

343 2020). Conversely, our estimated total CO<sub>2</sub> emission from 2012 to 2020 (165 Tg) was

344 lower than that (344 Tg) estimated by Liu et al. (2022), the latter was based on a

345 modified FRP algorithm and fire spot products by VIIRS, which has limitations in its

346 traditional straw extraction methods in accurately identifying fire spots during certain



347 times of the year (**Fig. 1(b)**). Therefore, integrating crop cycle information into fire spot  
348 extraction and classification methods is critical to enhance the accuracy of emission  
349 inventories.

### 350 **3.3 Driving factors of open straw burning**

351 Open straw burning is more prominently influenced by anthropogenic activities  
352 compared to other types of open biomass burning, such as forest, shrubland, and  
353 grassland fires (Syphard et al., 2017; Wu et al., 2020). Open straw burning is influenced  
354 by changes in straw yield and utilization rate, straw burning ban policy, and farmers'  
355 awareness of straw burning consequences (Chen et al., 2016; Li et al., 2017; Tao et al.,  
356 2018; Fang et al., 2019; Xu et al., 2023b).

357

358 Northeast China has experienced a remarkable expansion in its sown area for major  
359 grain crops over the past two decades. By 2020, the sown area reached 231,937 km<sup>2</sup>,  
360 61.4% more than that in 2001 (National Bureau of Statistics of China, 2002-2021). In  
361 the meantime, annual straw yield reached 143 Tg in 2020, 142% higher than that (59.2  
362 Tg) in 2001 (**Fig.6**) (numbers are calculated based on the major grain yields in  
363 Northeast China presented in National Bureau of Statistics of China (2002-2021) and  
364 the ratio of straw and grain (Wang et al.,2012)). Note that the annual straw yields have  
365 stabilized around 140 Tg since 2017, and this trend is expected to persist for many years  
366 to come (**Fig. 6**). From 2001 to 2020, a strong positive correlation was observed  
367 between the straw yields and the emissions of CO<sub>2</sub>-eq from open straw burning across



368 Northeast China, as well as in Heilongjiang and Jilin provinces ( $p < 0.01$ , **Table S2**). If  
369 looking at individual periods, significant correlations were only observed during  
370 **Period I** for the whole of Northeast China ( $p < 0.01$ ), as well as for Heilongjiang ( $p <$   
371  $0.01$ ), Jilin ( $p < 0.01$ ) and Liaoning provinces ( $p < 0.05$ ) (**Table S2**). This highlights  
372 that increased straw yields exacerbated the challenges of straw disposal in Northeast  
373 China and have been a major contributor to the increase in the emissions of GHGs from  
374 open straw burning in the aforementioned region and period.

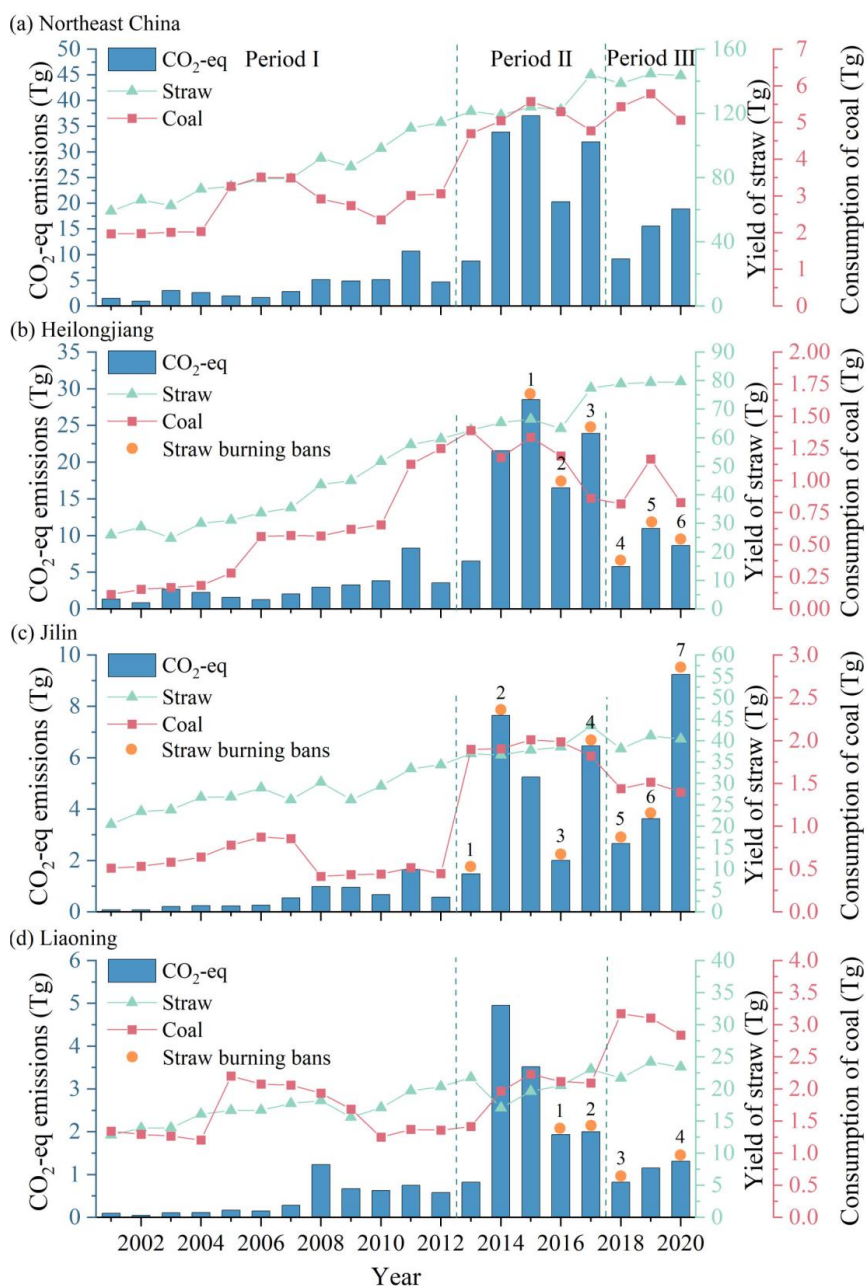
375

376 Besides open burning, crop straw is also used for cooking and heating in rural  
377 households in Northeast China (Ke et al., 2023; Liu et al., 2023). Crop straw can also  
378 be converted to bioenergy, used as animal feed, and returned to the fields (Alengebawy  
379 et al., 2022; Fang et al., 2022). However, exact quantification of straw utilization in  
380 different sectors in Northeast China is still lacking (Shi et al., 2023). Knowing that coal  
381 combustion and straw burning are major energy sources for rural households in  
382 Northeast China, we tried to explore potential changes in straw utilization on open straw  
383 burning through coal consumption changes (Fang et al. 2019). The abrupt increase in  
384 rural residential coal consumption in 2013 in Northeast China coincided with a spike in  
385 CO<sub>2</sub>-eq emissions from open straw burning (**Fig. 6(a)**). Furthermore, a significant  
386 positive correlation between rural residential coal consumption and CO<sub>2</sub>-eq emissions  
387 in Northeast China was revealed, especially in Heilongjiang and Jilin provinces (**Table**  
388 **S3**). We thus speculate that the increase in rural commercial energy consumption may





389 have reduced the demand for straw as an energy source for agricultural households,  
 390 thus facilitating the increased open straw burning. This needs to be confirmed in future  
 391 studies once various straw utilization pathways are quantified.



392



393 **Fig. 6** Annual CO<sub>2</sub>-eq emissions, yield of straw, rural residential coal consumption, and straw  
394 burning bans in (a) Northeast China, (b) Heilongjiang, (c) Jilin, and (d) Liaoning from 2001 to  
395 2020.

396

397 We also evaluated the efficacy of straw burning ban policy in Heilongjiang, Jilin, and  
398 Liaoning (**Table S4**). Despite the implementation of the policy since 2013 in this region,  
399 a significant reduction in CO<sub>2</sub>-eq emissions from open straw burning was only observed  
400 after 2018 (**Fig. 6**). Compared to the other regions of China, the effective control of  
401 open straw burning was delayed by several years in Northeast China (Huang et al.,  
402 2021). An important phenomenon was observed regarding the geographical and  
403 temporal expansion of the ban policy, e.g., initially focused on key areas and specific  
404 seasons (autumn and winter) and progressively extended to the entire region and  
405 throughout the whole year. (see Heilongjiang Province as an example, **Table S4**).  
406 Therefore, enhanced enforcement of the ban policy likely reduced CO<sub>2</sub>-eq emissions  
407 during **Period III** and shifted the burning season to spring.

408

409 In conclusion, the enforcement of region-specific straw burning bans tailored to  
410 spatiotemporal variations is crucial to control GHGs emissions, given the anticipated  
411 sustained high straw yields in the future. Additionally, promoting diverse methods for  
412 utilizing straw is highlighted as an effective strategy for mitigating carbon emissions  
413 resulted from open straw burning in Northeast China. A combined effort on policy



414 enforcement and alternative straw usage would play a pivotal role in addressing the  
415 environmental challenges posed by agricultural practices in the region.

416

#### 417 **4 Conclusions**

418 This study provides a comprehensive analysis of the spatiotemporal variations of open  
419 straw burning across Northeast China from 2001 to 2020 and develops regional scale  
420 high spatial resolution annual emission inventories of GHGs. Open straw burning in  
421 Northeast China emitted a total of 221 Tg of CO<sub>2</sub>-eq during 2001-2020, of which 20.4%  
422 was from **Period I** (2001-2012), 59.8% from **Period II** (2013-2017), and 19.8% from  
423 **Period III** (2018-2020). Analysis results demonstrate the necessity of integrating the  
424 crop cycle information into the extraction and classification of fire spots from open  
425 straw burning to enhance the accuracy of emission inventories of various pollutants.  
426 This study also highlights the inconsistencies between the number of fire spots and  
427 pollutant emissions caused by remote sensing detection techniques. In Northeast China,  
428 regions such as the northern Sanjiang Plain, eastern and northern Songnen Plain, and  
429 eastern Liao River Plain are identified as high-emission areas of GHGs from open straw  
430 burning, which emitted 38.9, 49.0, 33.3, and 12.2 Tg of CO<sub>2</sub>-eq, respectively, during  
431 2001-2020. Additionally, it is observed that the season for open straw burning has  
432 shifted from autumn to spring, with dispersed burning dates. This spatiotemporal  
433 analysis provides crucial insights into policy effectiveness as well as geographical



434 variations regarding compliance with regulations banning open straw burning.  
435 Consequently, government policies prohibiting open straw burning should be adjusted  
436 according to the observed spatiotemporal variations in different regions.  
437 Simultaneously promoting diversified applications of straw, such as bioenergy  
438 conversion, animal feeding, and soil amendment, is recommended — a strategy that is  
439 aligned with China’s dual-carbon objectives aiming at achieving carbon peak and  
440 carbon neutrality.

#### 441 **Data availability**

442 All raw data can be provided by the corresponding authors upon request.

#### 443 **Supplement**

444 The supplement related to this article is available online at:

445

#### 446 **Author contributions**

447 SC designed the research. ZS, LZ, CT, and QF developed the methodology. ZS

448 performed the formal analysis and wrote the initial draft. All the authors reviewed and

449 edited the draft.

450

#### 451 **Competing interests**

452 One of our co-authors is a member of the Editorial Board of ACP.



453 **Disclaimer**

454 Publisher's note: Copernicus Publications remains neutral with regard to jurisdictional  
455 claims made in the text, published maps, institutional affiliations, or any other  
456 geographical representation in this paper. While Copernicus Publications makes every  
457 effort to include appropriate place names, the final responsibility lies with the authors.

458

459 **Acknowledgments**

460 This work was supported by the Distinguished Youth Science Foundation of  
461 Heilongjiang Province (JQ2023E001) and Young Leading Talents of Northeast  
462 Agricultural University.

463

464 **References**

465 Ahmed, W., Tan, Q., Ali, S., and Ahmad, N.: Addressing environmental implications of  
466 crop stubble burning in Pakistan: innovation platforms as an alternative approach, Int.  
467 J. Global Warming, 19, 76-93, <https://doi.org/10.1504/IJGW.2019.101773>, 2019.

468 Alengebawy, A., Mohamed, B.A., Ran, Y., Yang, Y., Pezzuolo, A., Samer, M., and Ai,  
469 P.: A comparative environmental life cycle assessment of rice straw-based bioenergy  
470 projects in China, Environ. Res., 212, 113404,  
471 <https://doi.org/10.1016/j.envres.2022.113404>, 2022.

472 Chen, Y.L., Shen, H.Z., Zhong, Q.R., Chen, H., Huang, T.B., Liu, J.F., Cheng, H.F.,



473 Zeng, E.Y., Smith, K.R., and Tao, S.: Transition of household cookfuels in China from  
474 2010 to 2012, *Appl. Energ.*, 184, 800-809,  
475 <https://doi.org/10.1016/j.apenergy.2016.07.136>, 2016.

476 Cui, S., Song, Z.H., Zhang, L.M., Shen, Z.X., Hough, R., Zhang, Z.L., An, L.H., Fu,  
477 Q., Zhao, Y.C., and Jia, Z.Y.: Spatial and temporal variations of open straw burning  
478 based on fire spots in northeast China from 2013 to 2017, *Atmos. Environ.*, 244, 117962,  
479 <https://doi.org/10.1016/j.atmosenv.2020.117962>, 2021.

480 Fang, Y.R., Wu, Y., and Xie, G.H.: Crop residue utilizations and potential for bioethanol  
481 production in China, *Renew. Sust. Energ. Rev.*, 113, 109288,  
482 <https://doi.org/10.1016/j.rser.2019.109288>, 2019.

483 Fang, Y.R., Zhang, S.L., Zhou, Z.Q., Shi, W.J., and Xie, G.H.: Sustainable development  
484 in China: Valuation of bioenergy potential and CO<sub>2</sub> reduction from crop straw, *Appl.*  
485 *Energ.*, 322, 119439, <https://doi.org/10.1016/j.apenergy.2022.119439>, 2022.

486 Freeborn, P.H., Wooster, M.J., Hao, W.M., Ryan, C.A., Nordgren, B.L., Baker, S.P., and  
487 Ichoku, C.: Relationships between energy release, fuel mass loss, and trace gas and  
488 aerosol emissions during laboratory biomass fires, *J. Geophys. Res-Atmos.*, 113,  
489 D01301, <https://doi.org/10.1029/2007JD008679>, 2008.

490 Fu, J., Song, S.T., Guo, L., Chen, W.W., Wang, P., Duanmu, L.J., Shang, Y.J., Shi, B.W.,  
491 and He, L.Y.: Interprovincial joint prevention and control of open straw burning in  
492 Northeast China: Implications for atmospheric environment management, *Remote*  
493 *Sens.*, 14(11), 2528, <https://doi.org/10.3390/rs14112528>, 2022.



494 Gadde, B., Bonnet, S., Menke, C., and Garivait, S.: Air pollutant emissions from rice  
495 straw open field burning in India, Thailand and the Philippines, *Environ. Pollut.*, 157,  
496 1554-1558, <https://doi.org/10.1016/j.envpol.2009.01.004>, 2009.

497 Giglio, L., Schroeder, W., and Justice, C.O.: The collection 6 MODIS active fire  
498 detection algorithm and fire products, *Remote Sens. Environ.*, 178, 31-41,  
499 <https://doi.org/10.1016/j.rse.2016.02.054>, 2016.

500 Guan, Y.N., Chen, G.Y., Cheng, Z.J., Yan, B.B., and Hou, L.A.: Air pollutant emissions  
501 from straw open burning: A case study in Tianjin, *Atmos. Environ.*, 171, 155-164,  
502 <https://dx.doi.org/10.1016/j.atmosenv.2017.10.020>, 2017.

503 Hong, X., Zhang, C., Tian, Y., Wu, H., Zhu, Y., and Liu, C.: Quantification and  
504 evaluation of atmospheric emissions from crop residue burning constrained by satellite  
505 observations in China during 2016-2020, *Sci. Total. Environ.*, 865, 161237,  
506 <https://doi.org/10.1016/j.scitotenv.2022.161237>, 2023.

507 Huang, K., Zhuang, G., Lin, Y., Wang, Q., Fu, J.S., Fu, Q., Liu, T., and Deng, C.: How  
508 to improve the air quality over megacities in China: pollution characterization and  
509 source analysis in Shanghai before, during, and after the 2010 World Expo, *Atmos.*  
510 *Chem. Phys.*, 13, 5927-5942, <https://doi.org/10.5194/acp-13-5927-2013>, 2013.

511 Huang, L., Zhu, Y.H., Liu, H.Q., Wang, Y.J., Allen, D.T., Ooi, M.C.G.,  
512 Manomaiphiboon, K., Latif, M.T., Chan, A., and Li, L.: Assessing the contribution of  
513 open crop straw burning to ground-level ozone and associated health impacts in China  
514 and the effectiveness of straw burning bans, *Environ. Int.*, 171, 107710,



- 515 <https://doi.org/10.1016/j.envint.2022.107710>, 2023.
- 516 Huang, L., Zhu, Y.H., Wang, Q., Zhu, A.S., Liu, Z.Y., Wang, Y.J., Allen, D.T., and Li,  
517 L.: Assessment of the effects of straw burning bans in China: Emissions, air quality,  
518 and health impacts, *Sci. Total Environ.*, 789, 147935,  
519 <https://doi.org/10.1016/j.scitotenv.2021.147935>, 2021.
- 520 Huang, X., Li, M.M., Li, J.F., and Song, Y.: A high-resolution emission inventory of  
521 crop burning in fields in China based on MODIS Thermal Anomalies/Fire products,  
522 *Atmos. Environ.*, 50, 9-15, <https://doi.org/10.1016/j.atmosenv.2012.01.017>, 2012.
- 523 Jin, Q., Ma, X., Wang, W., Yang, S., and Guo, F.: Temporal and spatial variations of  
524 PM<sub>2.5</sub> emissions from crop straw burning in eastern China during 2000-2014. *Acta Sci.*  
525 *Circumstantiae*, 37, 460-468, 2017. (in Chinese)
- 526 Jin, Q.F., Ma, X.Q., Wang, G.Y., Yang, X.J., and Guo, F.T.: Dynamics of major air  
527 pollutants from crop residue burning in mainland China, 2000-2014, *J. Environ. Sci.*,  
528 70, 190-205, <https://doi.org/10.1016/j.jes.2017.11.024>, 2018.
- 529 Ke, H.B., Gong, S.L., He, J.J., Zhou, C.H., Zhang, L., and Zhou, Y.K.: Spatial and  
530 temporal distribution of open bio-mass burning in China from 2013 to 2017, *Atmos.*  
531 *Environ.*, 210, 156-165, <https://doi.org/10.1016/j.atmosenv.2019.04.039>, 2019.
- 532 Ke, Y.X., Zhang, F.X., Zhang, Z.L., Hough, R., Fu, Q., Li, Y.F., and Cui, S.: Effect of  
533 combined aging treatment on biochar adsorption and speciation distribution for Cd (II),  
534 *Sci. Total Environ.*, 867, 161593, <http://doi.org/10.1016/j.scitotenv.2023.161593>, 2023.
- 535 Korontzi, S., McCarty, J., Loboda, T., Kumar, S., and Justice, C.: Global distribution of





536 agricultural fires in croplands from 3 years of Moderate Resolution Imaging  
537 Spectroradiometer (MODIS) data, *Global Biogeochem. Cy.*, 20, GB2021,  
538 <https://doi.org/10.1029/2005GB002529>, 2006.

539 Li, C.L., Hu, Y.J., Zhang, F., Chen, J.M., Ma, Z., Ye, X.N., Yang, X., Wang, L., Tang,  
540 X.F., Zhang, R.H., Mu, M., Wang, G.H., Kan, H.D., Wang, X.M., and Mellouki, A.:  
541 Multi-pollutant emissions from the burning of major agricultural residues in China and  
542 the related health-economic effects, *Atmos. Chem. Phys.*, 17, 4957-4988,  
543 <https://doi.org/10.5194/acp-17-4957-2017>, 2017.

544 Li, L., Zhao, Q.Y., Zhang, J., Li, H.P., Liu, Q., Li, C.Y., Chen, F., Qiao, Y.Z., and Han,  
545 J.Z.: Bottom-up emission inventories of multiple air pollutants from open straw burning:  
546 A case study of Jiangsu province, Eastern China, *Atmos. Pollut. Res.*, 10, 501-507,  
547 <https://doi.org/10.1016/j.apr.2018.09.011>, 2019.

548 Li, X.H., Wang, S.X., Duan, L., Hao, J.M., Li, C., Chen, Y.S., and Yang, L.: Particulate  
549 and trace gas emissions from open burning of wheat straw and corn stover in China,  
550 *Environ. Sci. Technol.*, 41(17), 6052-6058, <https://doi.org/10.1021/es0705137>, 2007.

551 Li, X.Y., Yu, L., Peng, D.L., and Gong, P.: A large-scale, long time-series (1984-2020)  
552 of soybean mapping with phenological features: Heilongjiang Province as a test case,  
553 *Int. J. Remote Sens.*, 42, 7332-7356, <https://doi.org/10.1080/01431161.2021.1957177>,  
554 2021.

555 Liu, L.H., Jiang, J.Y., and Zong, L.G.: Emission inventory of greenhouse gases from  
556 agricultural residues combustion: A case study of Jiangsu Province, *Environ. Sci.*, 32,



- 557 1242-1248, 2011. (In Chinese)
- 558 Liu, Y.X., Zhao, H.M., Zhao, G.Y., Zhang, X.L., and Xiu, A.J.: Carbonaceous gas and  
559 aerosol emissions from biomass burning in China from 2012 to 2021, *J. Clean. Prod.*,  
560 362, 132199, <https://doi.org/10.1016/j.jclepro.2022.132199>, 2022.
- 561 Liu, Y.Z., Zhang, J., and Zhuang, M.H.: Bottom-up re-estimations of greenhouse gas  
562 and atmospheric pollutants derived from straw burning of three cereal crops production  
563 in China based on a national questionnaire, *Environ. Sci. Pollut. Res.*, 28, 65410-65415,  
564 <https://doi.org/10.1007/s11356-021-15658-9>, 2021.
- 565 Liu, Z.K., Cui, S., Fu, Q., Zhang, F.X., Zhang, Z.L., Hough, R., An, L.H., Li, Y.F., and  
566 Zhang, L.M.: Transport of neonicotinoid insecticides in a wetland ecosystem: has the  
567 cultivation of different crops become the major sources? *J. Environ. Manag.* 339,  
568 117838, <https://doi.org/10.1016/j.scitotenv.2023.161593>, 2023.
- 569 Luo, Y.C., Zhang, Z., Li, Z.Y., Chen, Y., Zhang, L.L., Cao, J., and Tao, F.L.: Identifying  
570 the spatiotemporal changes of annual harvesting areas for three staple crops in China  
571 by integrating multi-data sources. *Environ. Res. Lett.*, 15, 074003,  
572 <https://doi.org/10.1088/1748-9326/ab80f0>, 2020a.
- 573 Luo, Y.C., Zhang, Z., Chen, Y., Li, Z.Y., and Tao, F.L.: ChinaCropPhen1km: a high-  
574 resolution crop phenological dataset for three staple crops in China during 2000-2015  
575 based on leaf area index (LAI) products, *Earth Syst. Sci. Data*, 12, 197-214,  
576 <https://doi.org/10.5194/essd-12-197-2020>, 2020b.
- 577 Lv, Q.C., Yang, Z.Y., Chen, Z.Y., Li, M.C., Gao, B.B., Yang, J., Chen, X., and Xu, B.:



578 Crop residue burning in China (2019-2021): Spatiotemporal patterns, environmental  
579 impact, and emission dynamics, *Env. Sci. Ecotechnol.*, 21, 100394,  
580 <https://doi.org/10.1016/j.ese.2024.100394>, 2024.

581 Mehmood, K., Chang, S.C., Yu, S.C., Wang, L.Q., Li, P.F., Li, Z., Liu, W.P., Rosenfeld,  
582 D., Seinfeld, J.H.: Spatial and temporal distributions of air pollutant emissions from  
583 open crop straw and biomass burnings in China from 2002 to 2016, *Environ. Chem.*  
584 *Lett.*, 16, 301-309, <https://doi.org/10.1007/s10311-017-0675-6>, 2018.

585 Mehmood, K., Wu, Y.J., Wang, L.Q., Yu, S.C., Li, P.F., Chen, X., Li, Z., Zhang Y.B., Li,  
586 M.Y., Liu, W.P., Wang, Y.S., Liu, Z.R., Zhu, Y.N., Rosenfeld, D., and Seinfeld, J.H.:  
587 Relative effects of open biomass burning and open crop straw burning on haze  
588 formation over central and eastern China: modeling study driven by constrained  
589 emissions, *Atmos. Chem. Phys.*, 20, 2419-2443, [https://doi.org/10.5194/acp-20-2419-](https://doi.org/10.5194/acp-20-2419-2020)  
590 2020, 2020.

591 National Bureau of Statistics of China (NBSC): China Statistical Yearbook, China  
592 Statistics Press, Beijing, <http://www.stats.gov.cn/sj/ndsj/>, 2002-2021. (in Chinese)

593 Pan, X.L., Kanaya, Y., Taketani, F., Miyakawa, T., Inomata, S., Komazaki, Y., Tanimoto,  
594 H., Wang, Z., Uno, I., and Wang, Z.F.: Emission characteristics of refractory black  
595 carbon aerosols from fresh biomass burning: a perspective from laboratory experiments,  
596 *Atmos. Chem. Phys.*, 17, 13001-13016, <https://doi.org/10.5194/acp-17-13001-2017>,  
597 2017.

598 Peng, L.Q., Zhang, Q., and He, K.B.: Emissions inventory of atmospheric pollutants



599 from open burning of crop residues in China based on a national questionnaire, Res.  
600 Environ. Sci., 29, 1109-1118, 2016. (In Chinese)

601 Saxton, K.E., Kenny, J.F., and McCool, D.K.: Air permeability to define frozen soil  
602 infiltration with variable tillage and residue, Trans. ASABE, 36, 1369-1375,  
603 <https://dx.doi.org/10.13031/2013.28472>, 1993.

604 Schroeder, W., Oliva, P., Giglio, L., and Csiszar, I.A.: The New VIIRS 375 m active  
605 fire detection data product: Algorithm description and initial assessment, Remote Sens.  
606 Environ., 143, 85-96, <https://dx.doi.org/10.1016/j.rse.2013.12.008>, 2014.

607 Shi, W.J., Fang, Y.R., Chang, Y.Y., and Xie, G.H.: Toward sustainable utilization of crop  
608 straw: Greenhouse gas emissions and their reduction potential from 1950 to 2021 in  
609 China, Resour. Conserv. Recy., 190, 106824,  
610 <https://doi.org/10.1016/j.resconrec.2022.106824>, 2023.

611 Song, Z.H., Zhang, L.M., Tian, C.G., Li, K.Y., Chen, P.Y., Jia, Z.Y., Hu, P., and Cui,  
612 S.: Chemical characteristics, distribution patterns, and source apportionment of  
613 particulate elements and inorganic ions in snowpack in Harbin, China, Chemosphere,  
614 349, 140886, <https://doi.org/10.1016/j.chemosphere.2023.140886>, 2024.

615 Stavrakou, T., Müller, J.F., Bauwens, M., De Smedt, I., Lerot, C., Van Roozendaal, M.,  
616 Coheur, P.F., Clerbaux, C., Boersma, K.F. van der A, R., and Song, Y.: Substantial  
617 underestimation of post-harvest burning emissions in the North China plain revealed  
618 by multi-species space observations, Sci. Rep., 6, 32307,  
619 <https://dx.doi.org/10.1038/srep32307>, 2016.



620 Stockwell, C.E., Yokelson, R.J., Kreidenweis, S.M., Robinson, A.L., DeMott, P.J.,  
621 Sullivan, R.C., Reardon, J., Ryan, K.C., Griffith, D.W.T., and Stevens, L.: Trace gas  
622 emissions from combustion of peat, crop residue, domestic biofuels, grasses, and other  
623 fuels: configuration and Fourier transform infrared (FTIR) component of the fourth Fire  
624 Lab at Missoula Experiment (FLAME-4), *Atmos. Chem. Phys.*, 14, 9727-9754,  
625 <https://doi.org/10.5194/acp-14-9727-2014>, 2014.

626 Sun, J.F., Peng, H.Y., Chen, J.M., Wang, X.M., Wei, M., Li, W.J., Yang, L.X., Zhang,  
627 Q.Z., Wang, W.X., and Mellouki, A.: An estimation of CO<sub>2</sub> emission via agricultural  
628 crop residue open field burning in China from 1996 to 2013, *J. Clean. Prod.*, 112, 2625-  
629 -2631, <https://dx.doi.org/10.1016/j.jclepro.2015.09.112>, 2016.

630 Syphard, A.D., Keeley, J.E., Pfaff, A.H., and Ferschweiler, K.: Human presence  
631 diminishes the importance of climate in driving fire activity across the United States, *P.*  
632 *Natl. Acad. Sci. U.S.A.*, 114, 13750-13755, <https://doi.org/10.1073/pnas.1713885114>,  
633 2017.

634 Tang, R., Huang, X., Zhou, D.R., and Ding, A.J.: Biomass-burning-induced surface  
635 darkening and its impact on regional meteorology in eastern China, *Atmos. Chem.*  
636 *Phys.*, 20, 6177-6191, <https://doi.org/10.5194/acp-20-6177-2020>, 2020.

637 Tao, S., Ru, M.Y., Du, W., Zhu, X., Zhong, Q.R., Li, B.G., Shen, G.F., Pan, X.L., Meng,  
638 W.J., Chen, Y.L., Shen, H.Z., Lin, N., Su, S., Zhuo, S.J., Huang, T.B., Xu, Y., Yun, X.,  
639 Liu, J. F., Wang, X.L., Liu, W.X., Cheng, H.F., and Zhu, D.Q.: Quantifying the rural  
640 residential energy transition in China from 1992 to 2012 through a representative



641 national survey, *Nat. Energy*, 3, 567-573, <https://doi.org/10.1038/s41560-018-0158-4>,  
642 2018.

643 Tian, H., Zhao, D., and Wang, Y.: Emission inventories of atmospheric pollutants  
644 discharged from biomass burning in China, *Acta Sci. Circumstantiae*, 31, 349-357, 2011.  
645 (in Chinese)

646 Vadrevu, K., and Lasko, K.: Intercomparison of MODIS AQUA and VIIRS I-Band fires  
647 and emissions in an agricultural landscape-implications for air pollution research,  
648 *Remote Sens.*, 10, 978, <https://doi.org/10.3390/rs10070978>, 2018.

649 van der Werf, G.R., Randerson, J.T., Giglio, L., van Leeuwen, T.T., Chen, Y., Rogers,  
650 B.M., Mu, M.Q., van Marle, M.J.E., Morton, D.C., Collatz, G.J., Yokelson, R.J., and  
651 Kasibhatla, P.S.: Global fire emissions estimates during 1997-2016, *Earth Syst. Sci.*  
652 *Data*, 9, 697-720, <https://doi.org/10.5194/essd-9-697-2017>, 2017.

653 Vermote, E., Ellicott, E., Dubovik, O., Lapyonok, T., Chin, M., Giglio, L., and Roberts,  
654 G.J.: An approach to estimate global biomass burning emissions of organic and black  
655 carbon from MODIS fire radiative power, *J. Geophys. Res.*, 114, D18  
656 <https://doi.org/10.1029/2008jd011188>, 2009.

657 Wang, J.Y., Xi, F.M., Liu, Z., Bing, L.F., Alsaedi, A., Hayat, T., Ahmad., and Guan,  
658 D.D.: The spatiotemporal features of greenhouse gases emissions from biomass burning  
659 in China from 2000 to 2012, *J. Clean. Prod.*, 181, 801-808,  
660 <https://doi.org/10.1016/j.jclepro.2018.01.206>, 2018.

661 Wang, X.Y., Xue, S., and Xie, G.H.: Value-taking for residue factor as a parameter to



662 assess the field residue of field crops, *J. China Agr. Univ.*, 17.1, 1-8, 2012. (in Chinese)

663 Weldemichael, Y., and Assefa, G.: Assessing the energy production and GHG  
664 (greenhouse gas) emissions mitigation potential of biomass resources for Alberta, *J.*  
665 *Clean. Prod.*, 112, 4257-4264, <https://doi.org/10.1016/j.jclepro.2015.08.118>, 2016.

666 Wen, X., Chen, W.W., Chen, B., Yang, C.J., Tu, G., and Cheng, T.H.: Does the  
667 prohibition on open burning of straw mitigate air pollution? An empirical study in Jilin  
668 Province of China in the post-harvest season, *J. Environ. Manage.*, 264, 110451,  
669 <https://doi.org/10.1016/j.jenvman.2020.110451>, 2020.

670 Wooster, M.J., Roberts, G., Perry, G.L.W., and Kaufman, Y.J.: Retrieval of biomass  
671 combustion rates and totals from fire radiative power observations: FRP derivation and  
672 calibration relationships between biomass consumption and fire radiative energy  
673 release, *J. Geophys. Res-Atmos.*, 110, D24311, <https://doi.org/10.1029/2005JD006318>,  
674 2005.

675 Wu, B.B., Li, J.H., Yao, Z.L., Li, X., Wang, W.J., Wu, Z.C., and Zhou, Q.:  
676 Characteristics and reduction assessment of GHG emissions from crop residue open  
677 burning in China under the targets of carbon peak and carbon neutrality, *Sci. Total*  
678 *Environ.*, 905, 167235, <https://doi.org/10.1016/j.scitotenv.2023.167235>, 2023.

679 Wu, J., Kong, S.F., Wu, F.Q., Cheng, Y., Zheng, S.R., Qin, S., Liu, X., Yan, Q., Zheng,  
680 H., Zheng, M.M., Yan, Y.Y., Liu, D.T., Ding, S., Zhao, D.L., Shen, G.F., Zhao, T.L., and  
681 Qi, S.H.: The moving of high emission for biomass burning in China: View from multi-  
682 year emission estimation and human-driven forces. *Environ. Int.*, 142, 105812,



683 <https://doi.org/10.1016/j.envint.2020.105812>, 2020.

684 Wu, J., Kong, S.F., Wu, F.Q., Cheng, Y., Zheng, S.R., Yan, Q., Zheng, H., Yang, G.W.,  
685 Zheng, M.M., Liu, D.T., Zhao, D.L., and Qi, S.H.: Estimating the open biomass burning  
686 emissions in central and eastern China from 2003 to 2015 based on satellite observation,  
687 *Atmos. Chem. Phys.*, 18, 11623-11646, <https://doi.org/10.5194/acp-18-11623-2018>,  
688 2018.

689 Xu, R.B., Ye, T.T., Yue, X., Yang, Z.Y., Yu, W.H., Zhang, Y.W., Bell, M.L., Morawska,  
690 L., Yu, P., Zhang, Y.X., Wu, Y., Liu, Y.M., Johnston, F., Lei, Y.D., Abramson, M.J., Guo,  
691 Y.M., and Li, S.S.: Global population exposure to landscape fire air pollution from 2000  
692 to 2019, *Nature*, 621, 521-529, <https://doi.org/10.1038/s41586-023-06398-6>, 2023a.

693 Xu, C., and You, C.: Agricultural expansion dominates rapid increases in cropland fires  
694 in Asia, *Environ. Int.*, 179, <https://doi.org/108189>, [10.1016/j.envint.2023.108189](https://doi.org/10.1016/j.envint.2023.108189),  
695 2023b.

696 Xu, W.D., Wooster, M.J., Kaneko, T., He, J.P., Zhang, T.R., and Fisher, D.: Major  
697 advances in geostationary fire radiative power (FRP) retrieval over Asia and Australia  
698 stemming from use of Himarawi-8 AHI, *Remote Sens. Environ.*, 193, 138-149,  
699 <https://dx.doi.org/10.1016/j.rse.2017.02.024>, 2017.

700 Xuan, F., Dong, Y., Li, J.Y., Li, X.C., Su, W., Huang, X.D., Huang, J.X., Xie, Z.X., Li,  
701 Z.Q., Liu, H., Tao, W.C., Wen, Y.A., and Zhang, Y.: Mapping crop type in Northeast  
702 China during 2013-2021 using automatic sampling and tile-based image classification,  
703 *Int. J. Appl. Earth Obs.*, 117, 103178, <https://doi.org/10.1016/j.jag.2022.103178>, 2023.





- 704 Yang, G.Y., Zhao, H.M., Tong, D.Q., Xiu, A.J., Zhang, X.L., and Gao, C.: Impacts of  
705 post-harvest open biomass burning and burning ban policy on severe haze in the  
706 Northeastern China, *Sci. Total Environ.*, 716, 136517,  
707 <https://doi.org/10.1016/j.scitotenv.2020.136517>, 2020.
- 708 Yang, Y., and Zhao, Y.: Quantification and evaluation of atmospheric pollutant  
709 emissions from open biomass burning with multiple methods: a case study for the  
710 Yangtze River Delta region, China, *Atmos. Chem. Phys.*, 19, 327-348,  
711 <https://doi.org/10.5194/acp-19-327-2019>, 2019.
- 712 Zhang, X.H., Lu, Y., Wang, Q.G., and Qian, X.: A high-resolution inventory of air  
713 pollutant emissions from crop residue burning in China, *Atmos. Environ.*, 213, 207-214,  
714 <https://doi.org/10.1016/j.atmosenv.2019.06.009>, 2019.
- 715 Zhao, H.M., Yang, G.Y., Tong, D.Q., Zhang, X.L., Xiu, A.J., and Zhang, S.C.:  
716 Interannual and seasonal variability of greenhouse gases and aerosol emissions from  
717 biomass burning in Northeastern China constrained by satellite observations, *Remote  
718 Sens.*, 13, 1005, <https://doi.org/10.3390/rs13051005>, 2021.
- 719 Zheng, B., Ciais, P., Chevallier, F., Yang, H., Canadell, J.G., Chen, Y., van der Velde,  
720 I.R., Aben, I., Chuvieco, E., Davis, S.J., Deeter, M., Hong, C.P., Kong, Y.W., Li, H.Y.,  
721 Li, H., Lin, X., He, K.B., and Zhang, Q.: Record-high CO<sub>2</sub> emissions from boreal fires  
722 in 2021, *Science*, 379, 912-917, <https://doi.org/10.1126/science.ade0805>, 2023.
- 723 Zhou, Y., Xia, X.C., Lang, J.L., Zhao, B.B., Chen, D.S., Mao, S.S., Zhang, Y.Y., Liu, J.,  
724 and Li, J.: A coupled framework for estimating pollutant emissions from open burning



725 of specific crop residue: A case study for wheat, *Sci. Total Environ.*, 844, 156731,  
726 <https://doi.org/10.1016/j.scitotenv.2022.156731>, 2022.

727 Zhou, Y., Xing, X.F., Lang, J.L., Chen, D.S., Cheng, S.Y., Wei, L., Wei, X., and Liu, C.:  
728 A comprehensive biomass burning emission inventory with high spatial and temporal  
729 resolution in China, *Atmos. Chem. Phys.*, 17, 2839-2864, [https://doi.org/10.5194/acp-](https://doi.org/10.5194/acp-17-2839-2017)  
730 [17-2839-2017](https://doi.org/10.5194/acp-17-2839-2017), 2017.

731 Zhuang, Y., Li, R.Y., Yang, H., Chen, D.L., Chen, Z.Y., Gao, B.B., and He, B.:  
732 Understanding temporal and spatial distribution of crop residue burning in China from  
733 2003 to 2017 using MODIS data, *Remote Sens.*, 10(3), 390,  
734 <https://doi.org/10.3390/rs10030390>, 2018.

735 Zhu, C., Kawamura, K., and Kunwar, B.: Effect of biomass burning over the western  
736 North Pacific Rim: Wintertime maxima of anhydrosugars in ambient aerosols from  
737 Okinawa, *Atmos. Chem. Phys.*, 15, 1959-1973, [https://doi.org/10.5194/acp-15-1959-](https://doi.org/10.5194/acp-15-1959-2015)  
738 [2015](https://doi.org/10.5194/acp-15-1959-2015), 2015.